

## Original Article

# SLC25A18 has prognostic value in colorectal cancer and represses Warburg effect and cell proliferation via Wnt signaling

Li Liang<sup>1\*</sup>, Yanjie Chen<sup>2\*</sup>, Yiyi Yu<sup>1\*</sup>, Weiyu Pan<sup>3</sup>, Yuehong Cui<sup>1</sup>, Xiaojing Xu<sup>1</sup>, Ke Peng<sup>1</sup>, Mengling Liu<sup>1</sup>, Khalid Rashid<sup>1</sup>, Yingyong Hou<sup>3</sup>, Tianshu Liu<sup>1</sup>

Departments of <sup>1</sup>Medical Oncology, <sup>2</sup>Gastroenterology and Shanghai Institute of Liver Diseases, <sup>3</sup>Pathology, Zhongshan Hospital of Fudan University, NO. 180, Fenglin Road, Xuhui District, Shanghai 200032, China. \*Equal contributors.

Received March 4, 2020; Accepted April 23, 2020; Epub May 1, 2020; Published May 15, 2020

**Abstract:** Colorectal cancer (CRC) is a common malignant tumor worldwide. The solute carrier family 25 member 18 (SLC25A18) transports glutamate across the inner mitochondrial membrane and involves some non-tumor diseases, yet little is known about its role in malignancy. Here, we studied the function and mechanism of SLC25A18 in CRC. We conducted a bioinformatic analysis of the Cancer Genome Atlas (TCGA) and Gene Expression Omnibus (GEO) databases to identify the correlation of SLC25A18 expression with clinic-pathological characteristics. Function experiments were implemented to estimate the variation of aerobic glycolysis and cell proliferation due to *in vitro* and *in vivo* up- or down-regulation of SLC25A18. Immunohistochemical staining of SLC25A18 was performed on a tissue microarray of 106 patients with primary or metastatic CRC to evaluate its predictive and prognostic value. SLC25A18 expression was low in the CRC samples and was negatively correlated with stage, age and serum carcinoembryonic antigen levels. High expression of SLC25A18 indicated longer disease-free survival time after surgery. Exogenous overexpression of SLC25A18 decreased glucose consumption, lactate production, intracellular ATP concentration and cell proliferation and abrogated expression of CTNNB1, PKM2, LDHA and MYC. Inhibition of Wnt/ $\beta$ -catenin restored SLC25A18-repressed cellular activities. SLC25A18 clinically predicted a longer survival time after surgery or medicine treatment. These results showed that increased SLC25A18 expression inhibits Warburg effect and cell proliferation via Wnt/ $\beta$ -catenin cascade, and suggest a better prognosis after treatment.

**Keywords:** SLC25A18, Warburg effect, cell proliferation, Wnt/ $\beta$ -catenin, colorectal cancer, survival

## Introduction

About 1.5 million people have a history of invasive colorectal cancer (CRC) in the United States and over 1.2 million patients are living with CRC in 2019 [1, 2]. CRC is also the second most commonly diagnosed malignancy in Europe and the cause of tumor-related death in Europeans [3, 4]. In China, there were about 0.37 million newly diagnosed CRC cases, and about 0.19 million patients died of CRC in 2015 [5]. Advances in comprehensive therapeutic measures including surgery, chemotherapy and molecular therapy, have prolonged survival time or provided cure for some CRC patients. However, a large proportion of patients still suffer disease relapse or progression, following radical resections or effective

medicine therapy [6-9]. Several genes have been associated with CRC and a strong family history of CRC along with the presence of multiple polyps is an important genetic factor in the progression of CRC. Consequently, understanding the genetic process of the cancer recurrence and metastasis is of critical importance.

Human solute carrier families (SLCs), also known as mitochondrial transporter protein family [10], mediate solutes translocation from cytoplasm to mitochondria and are involved in metabolic reactions [11, 12]. SLC25A18 is a member of SLC25A family [13, 14], of which the mitochondrial carrier system is comprised [15]. Located on chromosome 22q11.21, SLC25A18 acts as a transporter of glutamate as well as H<sup>+</sup>

## SLC25A18 inhibits Warburg effect and proliferation

**Table 1.** Clinicopathological characteristics of 619 CRC cases from COAD and READ subsets in TCGA database

Clinic pathological characteristics	Number of cases (%)
<i>SLC25A18</i> expression	
High expressed	227 (36.7)
Low expressed	392 (63.3)
Primary Site	
Colon	449 (72.5)
Rectal	159 (25.7)
Missing	11 (1.8)
Histological type	
Colon Adenocarcinoma	387 (62.5)
Colon Mucinous Adenocarcinoma	62 (10.0)
Rectal Adenocarcinoma	146 (23.6)
Rectal Mucinous Adenocarcinoma	13 (2.1)
Missing	11 (1.8)
Gender	
Male	329 (53.2)
Female	290 (46.9)
Ethnicity	
White	292 (47.2)
Non-White	78 (12.6)
Missing	249 (40.2)
Pathologic T stage	
T1 and T2	125 (20.2)
T3 and T4	493 (79.6)
Missing	1 (0.2)
Pathologic N stage	
N0	351 (56.7)
N1 and N2	266 (43.0)
Missing	2 (0.3)
Pathologic M stage	
M0	459 (74.2)
M1	88 (14.2)
Missing	72 (11.6)
Microsatellite instability	
MSI	11 (1.8)
MSS	105 (17.0)
Missing	503 (81.3)
Residual tumor	
R0	451 (72.9)
R1 and R2	42 (6.8)
Missing	126 (20.4)
Survival status	
Alive	554 (89.5)
Dead	64 (10.3)
Missing	1 (0.2)

Vascular invasion	
Yes	132 (21.3)
No	405 (65.4)
Missing	82 (13.3)
Lymphatic invasion	
Yes	228 (36.8)
No	330 (53.3)
Missing	61 (9.9)
Perineural invasion	
Yes	60 (9.7)
No	171 (27.6)
Missing	338 (54.6)
Tumor deposits	
Yes	49 (7.9)
No	244 (39.4)
Missing	326 (52.7)
KRAS Mutation	
Yes	31 (5.0)
No	31 (5.0)
Missing	557 (90)
BRAF Mutation	
Yes	3 (0.5)
No	32 (5.2)
Missing	584 (94.4)
Mismatch repair protein present	
Yes	64 (10.3)
No	407 (65.8)
Missing	148 (23.9)

across the inner mitochondrial membrane [16-18]. *SLC25A18* is high expressed in the brain, liver and testis with relatively low expression in the breast, lung, colon and other tissues [19]. *SLC25A18* has been implicated in diseases such as cat eye syndrome, cutis laxa and maturity-onset diabetes of the young. Mutated *SLC25A18* is the cause of autosomal recessive disorder citrullinemia [20, 21]. Although *SLC25A18* is found in low expression in tumors compared with normal tissues [22], its role in CRC has not been investigated.

More than sixty years ago, Warburg proposed that cancer cells are distinguished from normal cells by their increased glucose utilization and lactate production even in the presence of oxygen and properly functioning mitochondria, which is later known as the Warburg effect [23]. Robert A. Weinberg [24] summarized that cancer cells widely feature energy reprogram-

## SLC25A18 inhibits Warburg effect and proliferation

**Table 2.** The relationship between SCL25A18 expression and clinicopathological characteristics of CRC cases from the TCGA database

Clinic pathological characteristics	Expression level of SLC25A18 mRNA		Number of cases	P-value
	High (%)	Low (%)		
Gender				
Male	213 (34.4)	116 (18.7)	619	0.4369
Female	179 (28.9)	111 (17.9)		
Primary Site				
Colon	290 (47.2)	163 (26.5)	615	0.5102
Rectal	99 (16.1)	63 (10.2)		
Histological type				
Colon Adenocarcinoma	248 (40.8)	139 (22.9)	608	0.4629
Colon Mucinous Adenocarcinoma	41 (6.7)	21 (3.5)		
Rectal Adenocarcinoma	86 (14.1)	60 (9.9)		
Rectal Mucinous Adenocarcinoma	10 (1.6)	3 (0.5)		
Ethnicity				
White	130 (35.1)	162 (43.8)	370	0.8831
Non-White	34 (9.2)	44 (11.9)		
Pathologic T stage				
T1 and T2	96 (15.5)	29 (4.7)	618	0.0004****
T3 and T4	295 (47.7)	198 (32)		
Pathologic N stage				
N0	234 (37.9)	117 (18.9)	617	0.0401**
N1 and N2	156 (25.2)	110 (17.8)		
Pathologic M stage				
M0	301 (55.0)	158 (28.9)	547	0.8844
M1	57 (10.4)	31 (5.7)		
Microsatellite instability				
MSI	5 (4.3)	6 (5.2)	116	0.9869
MSS	48 (41.4)	57 (49.1)		
Residual tumor				
R0	307 (62.3)	144 (29.2)	493	0.1595
R1 and R2	33 (6.7)	9 (1.8)		
Survival status				
Alive	355 (57.4)	199 (32.2)	618	0.3243
Dead	37 (6.0)	27 (4.4)		
Vascular invasion				
Yes	82 (15.3)	50 (9.3)	537	0.7824
No	257 (47.9)	148 (27.6)		
Lymphatic invasion				
Yes	160 (28.7)	68 (12.2)	558	0.0113**
No	197 (35.3)	133 (23.8)		
Perineural invasion				
Yes	23 (10.0)	37 (16.0)	231	0.4105
No	76 (32.9)	95 (41.1)		
Tumor deposits				
Yes	24 (8.2)	25 (8.5)	293	0.8540
No	116 (39.6)	128 (43.7)		
KRAS Mutation				

## SLC25A18 inhibits Warburg effect and proliferation

Yes	13 (21.0)	18 (29.0)	62	0.6020
No	11 (17.7)	20 (32.3)		
BRAF Mutation				
Yes	1 (2.9)	2 (5.7)	35	0.5460
No	6 (17.1)	26 (74.3)		
Mismatch repair protein present				
Yes	36 (7.6)	28 (5.9)	471	0.0072***
No	296 (62.8)	111 (23.6)		

Clinical data were investigated using chi-square test. \*\*P < 0.05; \*\*\*P < 0.01; \*\*\*\*P < 0.001.

ming of the regulators of “aerobic glycolysis”. Here, we studied the association between the *SLC25A18* expression and clinical treatment outcomes in CRC patients. We used information from TCGA and GEO databases, immunohistochemical examination of patients treated in our center, and *in vitro* and *in vivo* models to investigate the role and signal transduction of *SLC25A18* in tumor aerobic glycolysis. Our findings implicate *SLC25A18* as a novel therapeutic target for CRC.

### Materials and methods

#### Bioinformatics investigation of *SLC25A18*

To assess the expression level and clinical prognosis of *SLC25A18* in CRC, we used a GEPIA (Gene Expression Profiling Interactive Analysis) (<http://gepia.cancer-pku.cn/index.html>) and an UALCAN (Analyze, Integrate, Discover) (<http://ualcan.path.uab.edu/index.html>) online tools based on The Cancer Genome Atlas (TCGA) project of colon adenocarcinoma (COAD) and rectum adenocarcinoma (READ) (<https://portal.gdc.cancer.gov>) for bioinformatic investigation. Gene array expression data GSE14333 was downloaded from the GEO database (Gene Expression Omnibus) (<http://www.ncbi.nlm.nih.gov/geo>), which included 290 cases from surgically resected specimens of CRC. The patients enrolled in survival analysis were divided into high or low expression group according to the cut-off point of median transcripts per million (TPM) expression level and were compared by Log-rank test. The clinical pathological characteristics of cases from TCGA were further examined by R 3.6.1 (<https://www.r-project.org>) with TCGAbiolinks package.

#### Gene set enrichment analysis (GSEA)

To determine the biological function and signaling pathway associated with *SLC25A18* in-

volving, a gene set enrichment analysis (GSEA version 2.3.3, <http://www.broadinstitute.org/gsea/>) was implemented. Pre-defined gene set were retrieved from the Molecular Signatures Database, MSigDB (<http://software.broadinstitute.org/gsea/msigdb>). The thresholds for significance were determined by permutation analysis (1000 permutations) with default settings. False Discovery Rate (FDR) was then calculated. If the FDR score is less than 0.05, the gene set is considered significantly enriched.

#### Patients' recruitment and tissue samples

There were 106 cases of recurrence or metastatic CRC from Zhongshan Hospital affiliated to Fudan University included in this study. All study cases had been pathologically diagnosed as colorectal or metastatic hepatic cancer. The survival outcome and other clinic-pathological information such as gender, age, primary tumor location, *RAS/RAF* mutation status were recorded and presented in **Table 3**. This study was approved by the Institutional Review Board of Zhongshan Hospital affiliated to Fudan University. An informed consent was signed by all patients who agreed to participate in the studies.

#### Immunohistochemical (IHC) staining and evaluation

Tissue samples of patients with CRC were fixed in 10% formaldehyde, embedded in paraffin, cut into 4 to 7  $\mu\text{m}$  sections and attached onto glass slides. Tissues were deparaffinized with xylene, hydrophilized and unmasked following routine immunohistochemical procedure. The slides were blocked with 3% bovine serum albumin (BSA), and immune-stained with primary antibodies anti-*SLC25A18* (Proteintech, China, 17348-1-AP) at a dilution of 1:100 in a humidified box at 4°C overnight. Then, the slides were

## SLC25A18 inhibits Warburg effect and proliferation

**Table 3.** Characteristics of patients from a tissue microarray containing 106 primary or metastatic CRC tissues samples

Clinic pathological characteristics	Number of Cases (%)
Primary tumor site	
Colon	63 (59.4)
Rectum	43 (40.6)
Colon location	
Right	31 (29.2)
Left	75 (70.8)
Gender	
Male	74 (69.8)
Female	32 (30.2)
Age	
≤ 60	59 (55.7)
> 60	47 (44.3)
Initial stage	
Advanced	56 (52.8)
Recurrence	50 (47.2)
Survival statuses	
Death	50 (47.2)
Alive	56 (52.8)
Primary tumor resection	
Radical	56 (52.8)
Palliative	50 (47.2)
RAS status	
Mutated	58 (54.7)
Non mutated	48 (45.3)
RAF status	
Mutated	7 (6.6)
Non mutated	99 (93.4)
Anti EGFR therapy	
Yes	43 (40.6)
No	63 (59.4)
Anti-angiogenesis therapy	
Yes	56 (52.8)
No	50 (47.2)
Total	106 (100)

washed three times and incubated in the secondary antibody (1:400, Long ISLAND, BIOTEC CO., LTD, Shanghai, China) for 30 min at the room temperature. Thereafter, the slides were stained by 3,3'-diaminobenzidine (DAB) and counterstained by hematoxylin. Antigen-antibody complexes were visualized by micrograph analysis system (NIKON, Japan). Images of high cellularity area were taken and evaluated by color deconvolution with ImageJ software (Na-

tional Institutes of Health, Bethesda, MD). The intensity of the stain in cytoplasm was recorded as following: "negative" = 0; "weak" = 1; "moderate" = 2 and "strong" = 3. The percentage of positively stained cells in a section was recorded as 0% = 0, 1-24% = 1; 25-50% = 2; 51-75% = 3 and 76-100% = 4. The immunostaining score of was defined as the product of its intensity score obtained by adding individual positive percentage scores. Low *SLC25A18* expression referred to the immunostaining score ≤ 6, while high *SLC25A18* expression referred to the immunostaining score > 6.

### *RNA extraction, cDNA synthesis, and reverse transcription-quantitative polymerase chain reaction (RT-qPCR)*

For RT-qPCR examination, total RNA from the cell or tissue samples was extracted with TRIzol reagent (Invitrogen, USA), dissolved in RNase-free H<sub>2</sub>O and preserved at -80°C. cDNA was synthesized from each 1 µg RNA samples by Fermentas Reverse Transcription kit, followed by RT-PCR reactions on a real-time detector (ABI, ABI-7300, USA) using a SYBR Green PCR kit (Thermo, #K0223). The detailed steps were carried out as follows: pre-denaturation at 95°C for 10 min followed by 40 cycles of denaturation at 95°C for 15 sec, annealing at 60°C for 45 sec and elongation at 60°C for 60 sec. The primer sequences of *SLC25A18* and GAPDH were: *SLC25A18* forward, 5'-GTGTTCCCATCGACTTGG-3'; *SLC25A18* reverse, 5'-CAGGACCTGGCACATCC-3'; GAPDH forward, 5'-AATCCCATCACCATTTC-3' and GAPDH reverse, 5'-AGGCTGTGTCATACTTC-3'. The relative quantification of gene expression result was calculated by  $\Delta\Delta\text{CT}$ -method and expressed as  $2^{-\Delta\Delta\text{CT}}$  with setting glyceraldehyde-3-phosphatedehydrogenase (GAPDH) as the endogenous control.

### *Protein extraction, western blotting analysis, and antibodies*

For western blotting assays, cell lysates were arranged from cell lines with RIPA lysis buffer kit (JRDUN Biotechnology, Shanghai, China), and the protein concentrations were quantified with a BCA protein quantification kit (Thermo, Fisher Scientific, China). Equal amounts of protein (20 µg for cell samples and 50 µg for tissue samples) were separated onto sodium dodecyl sulfate polyacrylamide gel electropho-

## SLC25A18 inhibits Warburg effect and proliferation

resis (SDS-PAGE) and transferred to a polyvinylidene difluoride (PVDF) membrane. Membrane was incubated overnight at 4°C in primary antibodies diluted at 1:1000 in TBST buffer. Target proteins, include SLC25A18 (Proteintech, Wuhan, China, 17348-1-AP),  $\beta$ -catenin (Cell Signaling Technology, Danvers, MA, #95-87), c-Myc (Abcam, Cambridge, MA, Ab32072), PKM2 (Abcam, Ab137852), LHDA (Abcam, Ab125683), TCF4 (Affinity, DF6275), TCF1 (Affinity, DF7180), AKT1 (Cell Signaling Technology, Danvers, MA#2938), p-AKT1 (Cell Signaling Technology, #9081), and GAPDH (Cell Signaling Technology, #5174). The membrane was washed three times for 5 min each in TBST buffer to remove unbound primary antibodies. Incubation with HRP-conjugated goat anti-rabbit secondary antibodies IgG-HRP (Beyotime, Shanghai, China, A0208, A0216) for 60 min at room temperature was followed by another three washes with TBST buffer. Finally, blot signals were visualized by Tanon High-sig ECL (Tanon Science and Technology Co., Ltd., Shanghai, China). The expressing amount of each protein was semi-quantitatively identified and the densities of blots for all proteins were normalized to GAPDH.

### *Cell Lines and culture*

Five colorectal cancer cell lines (HCT116, HS675.T, LOVO, SW480, SW620) and one normal gastrointestinal epithelial cell line (HIEC) were purchased from the Cell Bank of Chinese Academy of Sciences. HCT116, HS675.T and SW620 cell lines were cultured in RPMI-1640. LOVO and SW480 cell lines were cultured in DMEM containing 10% fetal bovine serum and 1% double antibiotics (penicillin and streptomycin), and maintained in a humidified incubator with 5% CO<sub>2</sub> at 37°C.

### *Lentivirus construction and cell transduction*

In order to knockdown of *SLC25A18*, three human siRNA sequences (RNAi 1, GGCAGAGGTTCTTACCGAA; RNAi 2, GGATGCAGCGAA-CCTGAA; RNAi 3, GCGTTGTAGTGCTACCTCA) were synthesized by Genewiz Company (Shanghai, China) and cloned into a pLKO.1 vector. The DNA coding region (cDNA) of *SLC25A18* (NM\_031481.3) was also synthesized and cloned into a pLVX-Puro vector at EcoRI/BamHI restriction sites. The integrity of relevant core plasmids was verified by DNA sequencing (Majorbio, Shanghai). Next, the constructed plas-

mids (pLKO.1-sh*SLC25A18*, pLVX-Puro-*SLC25A18i*) and viral package plasmids (psPAX2, pMD2G) were co-transfected into 293T cells to generate relevant lentivirus; supernatants were collected after 48 h of infection. HS675.T, SW620, HCT116 and LOVO cell lines were seeded into 6-well plates overnight before transduction. After that, SW620 and HS675.T cell lines were infected with lentivirus containing *SLC25A18*-shRNAs or lenti-vector (NC) supernatants, while HCT116 and LOVO cell lines were treated with lenti-oe*SLC25A18*. Lentivirus at a multiplicity of infection (MOI) of 5 was added to cells at 70% confluency. After 48 h infection, the expression levels of *SLC25A18* mRNA and protein were checked by RT-PCR and western blotting.

### *Cell proliferation detection*

The cell proliferation rate was assessed by cell counting kit-8 (CCK-8) assay. Cells were plated onto 96-well microplates at a density of 1 to 5 × 10<sup>3</sup> cells per well, allowed to attach overnight in a humidified 5% CO<sub>2</sub> incubator at 37°C, and were observed periodically. At 0 h, 12 h, 24 h and 48 h after transfection, cells were treated with CCK-8 and incubated for 1 h at 37°C. The absorbance value (optical density, OD) of each well was measured at 450 nm by a microplate reader (Perlong, Beijing).

### *Glucose uptake analysis*

For detection of glucose consumption, the fluorescent glucose analog 2-((7-nitro-2,1,3-benzoxadiazol-4-yl) amino)-2-deoxyglucose (2-NBDG) (K682-50, Biovision) was used to assess cell glucose uptake. Cells were seeded and incubated for 24 h. Culture medium was removed replaced with phosphate buffer solution (PBS) containing 100  $\mu$ mol/L of the fluorescent glucose analog 2-NBDG for another one hour. Free 2-NBDG was washed out with cold PBS twice. Cells were then lysed with 0.25% trypsin-EDTA (Solarbio, China) and stained with 5 mg/mL propidium iodide (PI) for 30 min at 37°C, prior to detection by flow cytometry.

### *Extracellular lactate colorimetric assay*

The extracellular lactate level, as the end product of glycolysis, was measured using Lactate Colorimetric Assay Kit (Jiancheng Bioengineering, Inst, Nanjin), according to the manu-

## SLC25A18 inhibits Warburg effect and proliferation

facturer's protocol. For this, cells were seeded in 6-well plates, incubated and deproteinized. The optical density was measured at 450 nm. The standard curve (nmol/well vs. OD 450 nm) was plotted. Lactate concentrations were calculated according to the formula offered by the kit manufacturer as following: Lactic acid =  $(OD_{\text{test}} - OD_{\text{zero}}) / (OD_{\text{standard}} - OD_{\text{zero}}) \times \text{standard sample concentration} \times \text{sample dilution factor}$  (gort/L).

### Intracellular ATP assay

Intracellular ATP levels were measured with ATP Assay Kit (Jiancheng Bioengineering, Inst, Nanjin), according to manufacturer's instructions. In brief, cells were treated with ATP releasing reagent and then transferred to a flat white bottom 96-well plate. The optical density was measured at 636 nm. The standard curve (nmol/well vs. OD 636 nm) was plotted and the ATP calculated using the formula provided by the kit manufacturer:  $ATP = (OD_{\text{test}} - OD_{\text{control}}) / (OD_{\text{standard}} - OD_{\text{zero}}) \times \text{standard sample concentration} \times \text{sample dilution factor} / \text{protein concentration}$  (gort/L).

### In vivo assay of tumor growth and aerobic glycolysis in xenograft nude mice

A total of twelve female BALB/c nude mice with 4 to 6-week-old and 18 to 20 g of weight, were obtained from Shanghai Experimental Animal Center (Shanghai, China). Mice were raised in specific-pathogen-free (SPF) conditions and were divided randomly into two groups of six. These nude mice were subcutaneously injected with  $5 \times 10^6$  HCT116 cell line transduced with lenti-vector or lenti-oeSLC25A18. After subcutaneous injection, the nude mice were raised in cages, bred with water and feed. Lengths (L) and widths (W) of subcutaneous tumors were measured with a vernier caliper every 3 days after tumor formation. Then the mice were killed one month later and photographed. The tumors were taken out, weighed, and recorded. And the tumor volumes were calculated by the following formula:  $\text{volume} = (\text{length} \times \text{width}^2) \times 0.5$ . The tumor tissues were also formalin-fixed, paraffin-embedded, and hematoxylin-eosin (H&E) stained to evaluate SLC25A18 expression. The tumor lysates were assessed for SLC25A18 mRNA and protein expression levels by RT-PCR and western blotting respectively. All xenograft experiments were approved by the Animal Ex-

periments Ethics Committee of Zhongshan Hospital, Fudan University.

### Statistical analysis

Data were recorded as the mean  $\pm$  standard deviation (SD). The survival analysis was conducted using Kaplan Meier method and Log-rank test. Clinical data were investigated using chi-square test. A T-test was adopted to compare the two groups of data. Pairwise comparisons of the above single-factor groups were conducted by one-way ANOVA, and multiple comparisons were conducted by Dunnett's test. Two-way ANOVA was used for pairwise comparison of the above two factors, and Dunnett's test was used for multiple comparisons. Data were also analyzed by rank sum test and Spearman correlation test. The *P*-value less than 0.05 was considered significant.

## Results

### SLC25A18 presents as a tumor inhibitor and its downregulation suggests a worse clinical outcome

SLC25A18 mRNA level expresses low in CRC: To explore unreported genes positively or negatively related to patient prognosis, CRC cases from TCGA (COAD and READ) and GEO (GSE14333) databases were retrieved. According to the bioinformatics analysis, SLC25A18 was expressed lower levels in colon cancer samples than normal samples from TCGA database (Tumor, vs. normal, 275, vs. 41,  $P < 0.01$ ) or TCGA combined with GTEx databases (Tumor, vs. normal, 275, vs. 439,  $P < 0.001$ ); the median  $\text{Log}_2$  (TPM+1) for SLC25A18 mRNA expression in colon tumor samples and normal samples was 0.233, vs. 0.303 and 0.202, vs. 1.263. Further, we found that SLC25A18 was also expressed lower in rectal cancer samples in TCGA database (Tumor, vs. normal, 92, vs.10,  $P < 0.01$ ) or TCGA combined with GTEx databases (Tumor, vs. normal, 92, vs. 318,  $P < 0.001$ ); the median  $\text{Log}_2$  (TPM+1) for SLC25A18 mRNA expression in rectal tumor samples and normal samples was 0.225, vs. 0.462 and 0.202, vs. 1.263, respectively (**Figure 1A**). Additional investigation suggested that SLC25A18 expression was low in thirty-one matched tumor-para samples of patients with CRC (0.288, vs. 0.472,  $P < 0.0001$ , **Figure 1B**).

# SLC25A18 inhibits Warburg effect and proliferation

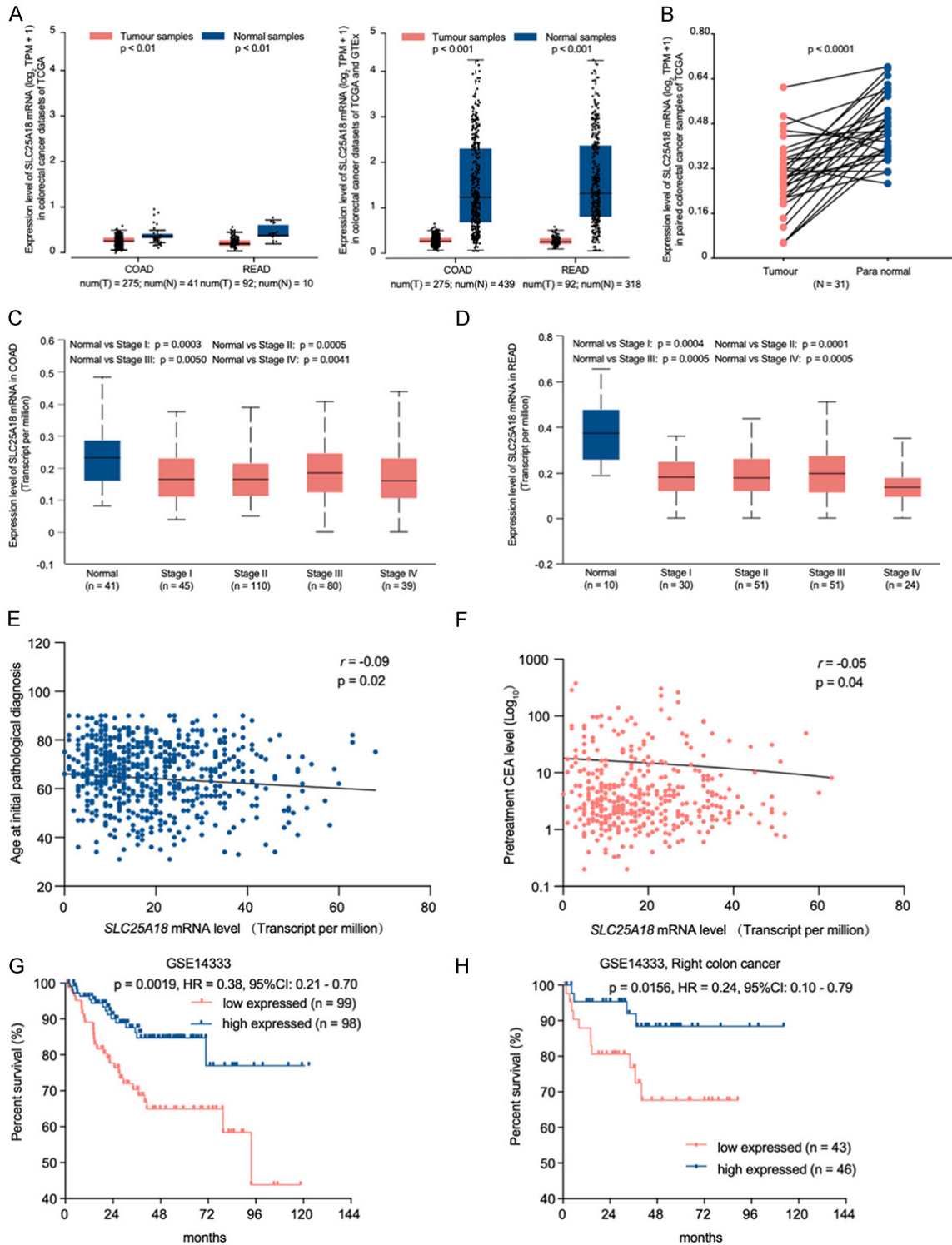


**Figure 1.** SLC25A18 expression in colorectal cancer (CRC) and indicates unfavorable clinicopathological characteristics and prognosis. A, B. SLC25A18 mRNA levels in CRC tissue were lower than not only normal tissue in colon adenocarcinoma (COAD) ( $N_{\text{tumour}} = 275$ ,  $N_{\text{normal}} = 41$ ) and rectum adenocarcinoma (READ) ( $N_{\text{tumour}} = 92$ ,  $N_{\text{normal}} = 10$ ) subsets from TCGA and GTEx ( $N_{\text{normal}} = 318$ ) database, but also in matched para-tumor tissues ( $N = 31$ ). C, D. SLC25A18 exhibited low expression in individual colon and rectum adenocarcinoma stages compared to normal tissue samples. E, F. SLC25A18 expression is negatively related to some clinical characteristics such as age and pretreatment serum carcinoembryonic levels (CEA). G, H. CRC patients with low expression of SLC25A18 exhibited a shorter disease-free survival time after receiving a radical surgery treatment, especially for those people with right colon cancer according to a cohort from GSE14333.

## SLC25A18 inhibits Warburg effect and proliferation

### *Low SLC25A18 mRNA level is related to aggressive clinic-pathological characteristics*

We used an online tool, UALCAN, to demonstrate that *SLC25A18* was downregulated in colon (**Figure 1C**) and rectal (**Figure 1D**) cancer cases of Stage I to IV when compared to normal cases individually. To further study the relationship between *SLC25A18* expression and clinic-pathological characteristics, a total of six hundred and nineteen cases with 449 colon cancer cases from COAD and 159 rectal cancer cases from READ were downloaded from TCGA datasets and listed in **Table 1**. When regrouped by median expression value, low expression of *SLC25A18* were found associated with advance pathologic T stage ( $X^2 = 12.34$ ,  $P = 0.0004$ ), N stage ( $X^2 = 4.18$ ,  $P = 0.0407$ ), more lymphatic invasion ( $X^2 = 6.42$ ,  $P = 0.0112$ ) and mismatch repair protein present ( $X^2 = 7.21$ ,  $P = 0.0072$ ) (**Table 2**). *SLC25A18* expression level was negatively related to age ( $r = -0.09$ ,  $P = 0.02$ , **Figure 1E**) and pretreatment serum carcinoembryonic antigen (pre-CEA) level ( $r = -0.05$ ,  $P = 0.04$ , **Figure 1F**)

### *Low SLC25A18 mRNA level indicates shorter disease-free survival time after radical surgery resection*

A survival survey for patients who experienced radical primary tumor resection was performed. According to GSE163333 dataset, patients with low *SLC25A18* expression experienced a shorter disease-free survival (HR = 0.38,  $P = 0.0019$ , **Figure 1G**), especially for that suffering right colon malignant disease (HR = 0.24,  $P = 0.0156$ , **Figure 1H**), which suggested that low *SLC25A18* expression indicated a higher recurrence risk.

### *SLC25A18 weakens the Warburg effect in CRC by attenuating cell glucose consumption, lactate production and ATP content*

To identify the function of *SLC25A18* in CRC cells, we investigated the aerobic glycolysis by means of glucose uptake assays, lactate production assays and ATP content assays. After evaluation of primary expression level (**Figure 2A**), HCT116, LOVO, SW620 and HS675.T with comparatively low or high *SLC25A18* expression were selected to establish *SLC25A18* overexpression or silencing cell models, respectively. The efficiency of overexpression and

knockdown was confirmed by RT-PCR and western blotting (**Figure 2B, 2C**). Flow cytometric data indicated lower glucose uptake in HCT116 and LOVO, in contrast to SW620 and HS675.T, which demonstrated higher glucose uptake (**Figure 2D**). *SLC25A18* overexpression decreased lactate production in HCT116 ( $2.534 \pm 0.008$  vs.  $6.447 \pm 0.034$  mmol/ $\mu$ g,  $P = 0.0003$ ) and LOVO ( $7.936 \pm 0.313$  vs.  $2.210 \pm 0.991$  mmol/ $\mu$ g,  $P = 0.0062$ ). However, silencing *SLC25A18* increased lactate levels in SW620 ( $13.590 \pm 0.268$  vs.  $7.162 \pm 0.175$  mmol/ $\mu$ g,  $P = 0.0015$ ) and HS675.T ( $13.870 \pm 0.456$  vs.  $7.344 \pm 0.294$   $\mu$ mol/ $\mu$ g,  $P = 0.0046$ ) (**Figure 2E**). Increase in ATP by aerobic glycolysis was observed in HCT116 ( $37.083 \pm 9.320$  vs.  $115.435 \pm 5.064$   $\mu$ mol/gprot,  $P = 0.0161$ ) and LOVO ( $45.274 \pm 6.553$  vs.  $137.467 \pm 12.476$   $\mu$ mol/gprot,  $P = 0.0106$ ) with overexpression of *SLC25A18*, while its silencing resulted in lower ATP levels in SW620 ( $214.563 \pm 18.339$  vs.  $118.507 \pm 7.017$   $\mu$ mol/gprot,  $P < 0.0001$ ) and HS675.T ( $202.406 \pm 9.891$  vs.  $107.572 \pm 11.509$   $\mu$ mol/gprot,  $P < 0.0001$ ) (**Figure 2F**).

### *SLC25A18 suppresses CRC cell proliferation*

To examine the influence of *SLC25A18* on CRC cell growth, we used CCK-8 assays. As shown in **Figure 2G**, upregulation of *SLC25A18* inhibited cell proliferation and its downregulation promoted cell growth after 72 h of infection, implying that *SLC25A18* can inhibit CRC proliferation in vitro.

### *SLC25A18 negatively regulates genes related to the Warburg effect as well as Wnt/ $\beta$ -catenin signaling pathway*

As suggested by **Figure 3A**, the protein level of pyruvate kinase M2 (*PKM2*), lactic dehydrogenase kinase-A (*LDHA*), myc proto-oncogene (*MYC*) and phosphorylated AKT serine/threonine kinase1 (*pAKT1*) were decreased or increased when *SLC25A18* was overexpressed or knocked down respectively, which indicated that *SLC25A18* may impede cell aerobic glycolysis and proliferation of CRC. To survey the *SLC25A18*-mediated biological process and signaling pathways in CRC progression, a GSEA analysis was performed on the CRC cases in TCGA database, stratified by *SLC25A18* median expression level. We found that gene sets, such as FEVR\_CTNNB1\_TARGETS\_DN, HALL-

## SLC25A18 inhibits Warburg effect and proliferation

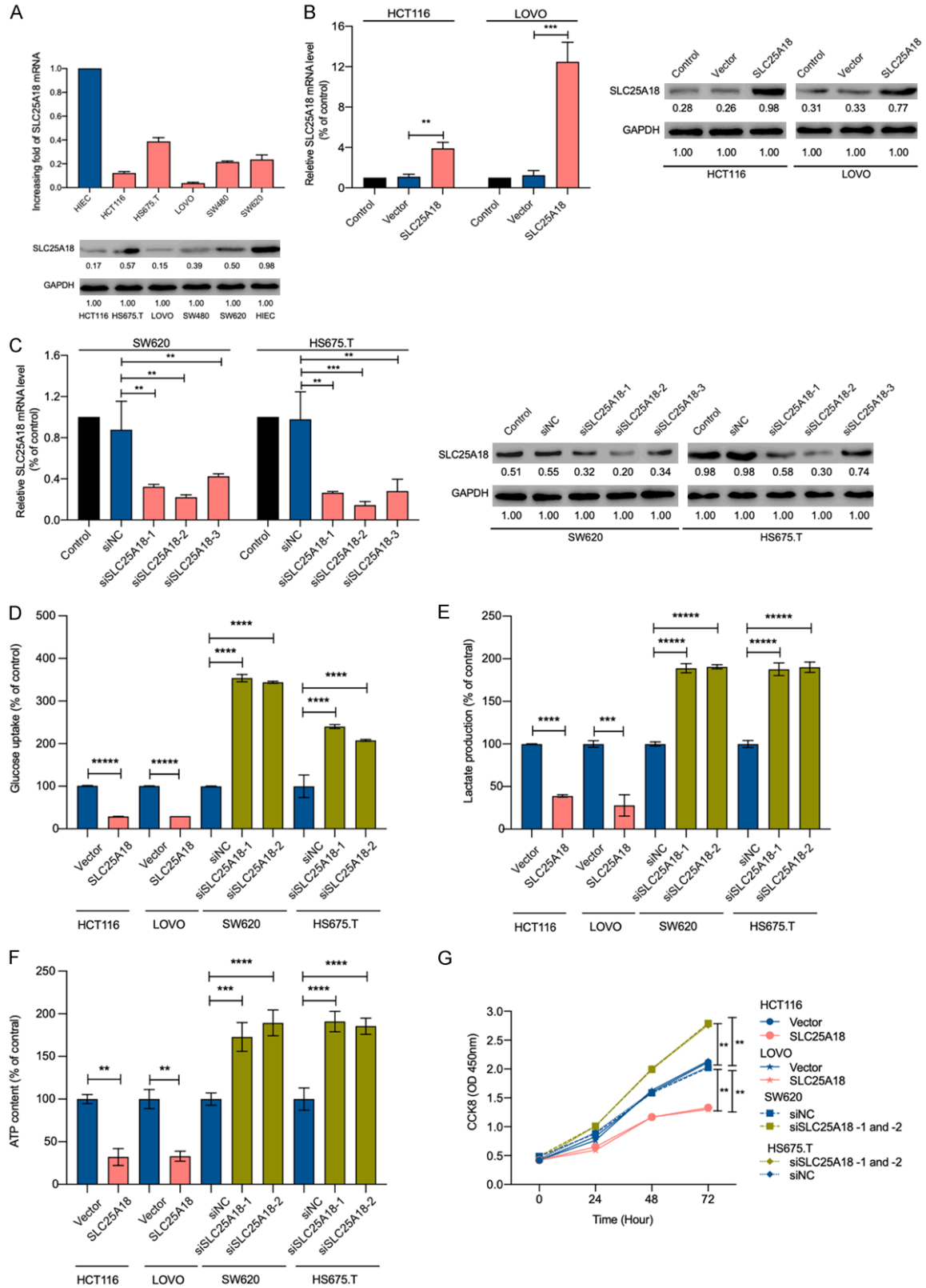
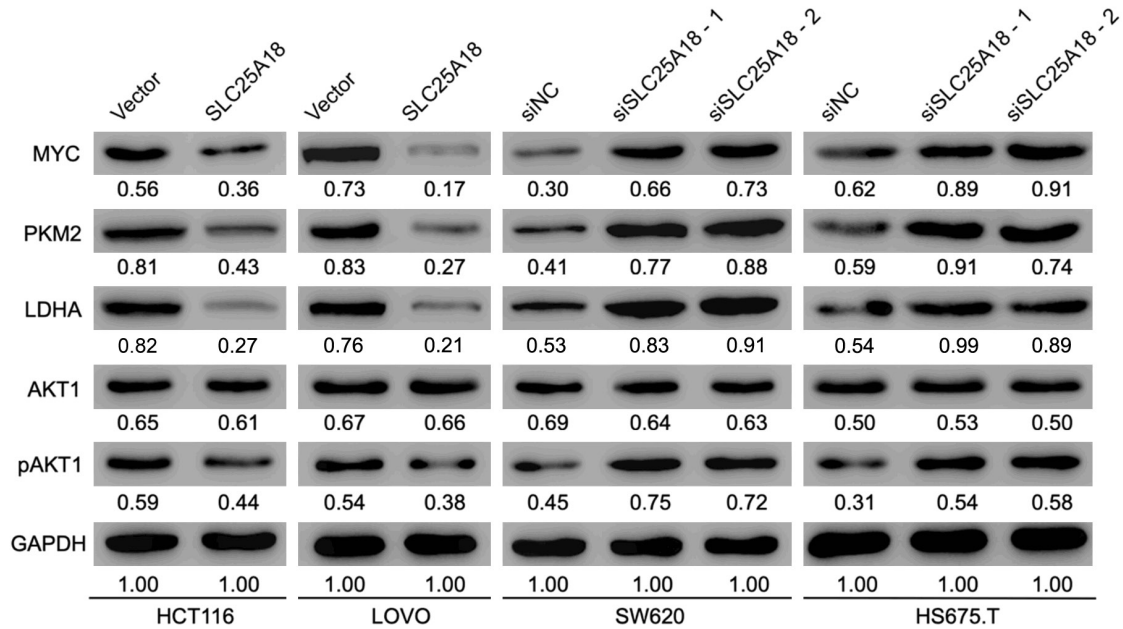


**Figure 2.** SLC25A18 attenuates CRC cell lines aerobic glycolysis and cell proliferation. A. The expression levels of SLC25A18 mRNA and protein in human CRC cell lines (HCT116, HS675.T, LOVO, SW480, SW620) and intestinal epithelial cell line (HIEC) were examined by RT-PCR and western blotting. B, C. The mRNA and protein levels of

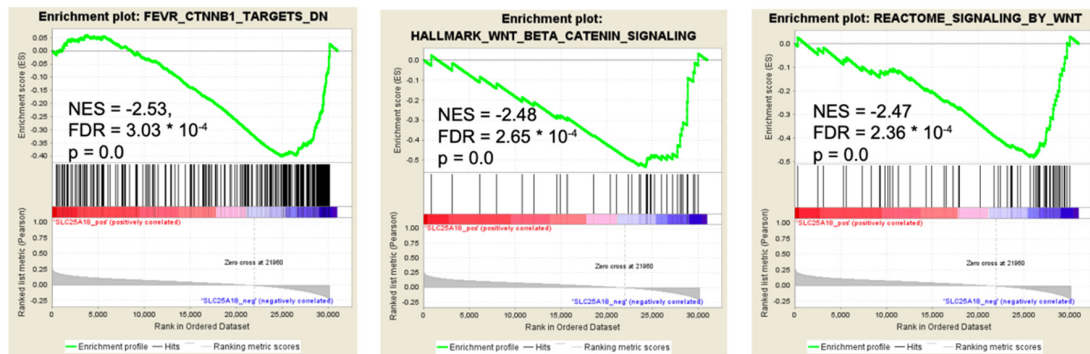
## SLC25A18 inhibits Warburg effect and proliferation

SLC25A18 were checked after 48 hours of infection with lentivirus to confirm the overexpressing and silencing efficiency in CRC cell lines, respectively. D-F. After transfection, flow cytometry analysis, extracellular lactate colorimetric test, and intracellular ATP content detection suggested a decrease in glucose uptake, lactate production, ATP generation, and an increase in that when SLC25A18 was overexpressed or silenced, respectively. G. Subsequently, CCK-8 assays at 0, 24, 48, and 72 h revealed the attenuation of cell viability and proliferation in HCT116, LOVO and enhancement of that in SW620 and HS675.T. All experiments were conducted in triplicates. Data are presented as mean  $\pm$  SD. \*\*,  $P < 0.05$ ; \*\*\*,  $P < 0.001$ ; \*\*\*\*,  $P < 1 \times 10^{-4}$ ; \*\*\*\*\*,  $P < 1 \times 10^{-5}$ .

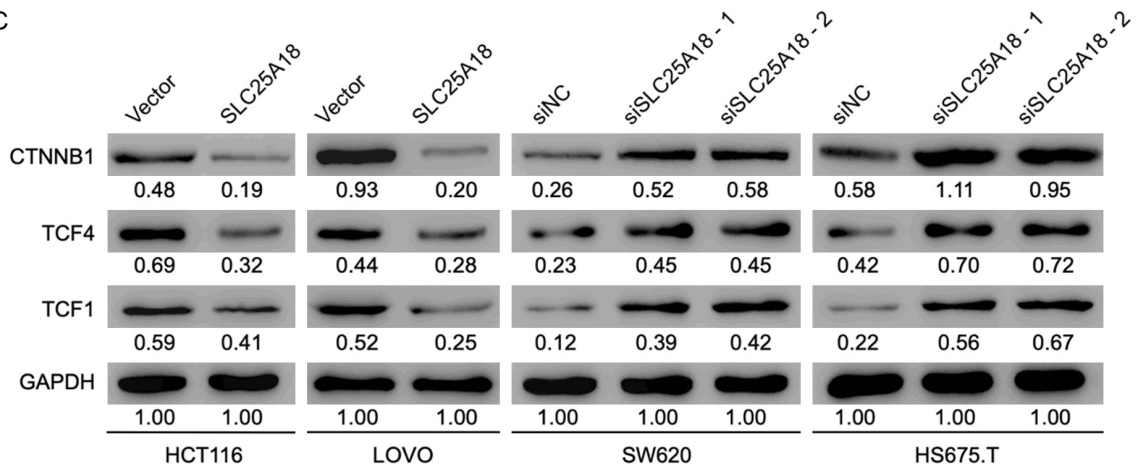
A



B



C



## SLC25A18 inhibits Warburg effect and proliferation

**Figure 3.** *SLC25A18* negatively regulates genes expression related to aerobics glycolysis, cell proliferation, and Wnt/ $\beta$ -catenin cascade. (A) Western blotting verified a negative protein level of genes such as *MYC*, *PKM2*, *LDHA*, *AKT1* and *pAKT1* which are involved in cell aerobics glycolysis and cell proliferation when *SLC25A18* was overexpressed or knocked down. (B) Gene set enrichment analysis implied a negative relationship between highly expressed *SLC25A18* and the enrichment of *CTNNB1* target genes and Wnt/ $\beta$ -catenin Signaling (HALLMARK\_WNT\_BETA\_CATENIN\_SIGNALING, REACTOME\_SIGNALING\_BY\_WNT) in patients with CRC from the TCGA database, (C) which was also verified by western blotting. All experiments were conducted in triplicates.

MARK\_WNT\_BETA\_CATENIN\_SIGNALING and REACTOME\_SIGNALING\_BY\_WNT, were significantly enriched in samples with low expressed *SLC25A18* or blue module (**Figure 3B**). Western blotting results showed that protein levels of catenin beta 1 (*CTNNB1*) and its targets, transcription factor 4 and 1 (*TCF4*, *TCF1*), were negatively regulated by *SLC25A18* (**Figure 3C**).

*SLC25A18* exerted functions depends on Wnt/ $\beta$ -catenin signaling pathway

To confirm biological effect of *SLC25A18*, we repeated the previous functional experiments after treating HS675.T with *SLC25A18* knock-down with 20  $\mu$ mol/L Wnt signaling pathway inhibitor (dickkopf inhibitor 1, *DKK1*) for 24 h. As shown in **Figure 4A-D**, *DKK1* decreased of cell glucose uptake, lactate production, and ATP levels, and weakened cell proliferation, reversing the enhancement of these functions propagated by *SLC25A18* knockdown. The protein levels of initially upregulated genes were also found decreased in the presence of *DKK1* (**Figure 4E**). These results unraveled a mechanism of *SLC25A18* actions that controls aerobic glycolysis and cell proliferation through the Wnt/ $\beta$ -catenin signaling pathway in CRC.

*SLC25A18* inhibits colorectal cancer aerobic glycolysis in xenograft nude mice

To confirm the effect from *SLC25A18* upregulation *in vivo*, transduced HCT116 were injected subcutaneously to establish the mice xenograft models. The tumors generated in all nude mice with macroscopically larger tumor mass at the injection site (**Figure 5A**). The tumor volume ( $214.71 \pm 74.09$  vs.  $609.76 \pm 134.87$  mm<sup>3</sup>,  $P < 0.0001$ ) and weight ( $0.14 \pm 0.04$  vs.  $0.38 \pm 0.07$  g,  $P < 0.0001$ ) were smaller in *SLC25A18* overexpressed group at about thirty-three days (**Figure 5B** and **5C**). The increase in expression of *SLC25A18* was verified in tissues by IHC staining evaluated for positive area ( $1141 \pm 339.5$  vs.  $682.3 \pm 110.8$

$\times 0.095$   $\mu$ m<sup>2</sup>,  $P = 0.0004$ ) (**Figure 5D**), as well as in tumor masses by RT-PCR (**Figure 5E**) and western blotting (**Figure 5F**). The protein levels of *CTNNB1*, *MYC*, *PKM2*, *LDHA* were also assessed as shown in **Figure 5F**. These results indicated that *SLC25A18* reduced tumor progression possibly by attenuating aerobic glycolysis in CRC.

*SLC25A18* upregulation in CRC patients who experience a longer survival time after surgery treatment or drug therapy

To identify the relationship between *SLC25A18* expression and patient's prognosis after surgery or medicine treatment, IHC staining and evaluation were performed in a tissue microarray containing 106 primary or metastatic CRC tissues samples (**Table 3**). The cohort was divided into two groups according to immunostaining scores of *SLC25A18* (**Table 4**). The representative IHC staining photographs of primary colorectal or metastatic hepatic tissues samples are shown in **Figure 6A**. We observed a negative expression relationship between *SLC25A18* and genes involving cell stemness or aerobic glycolysis: *SOX6* ( $r = -0.2515$ ,  $P = 0.0108$ ) and *MYC* ( $r = -0.3253$ ,  $P = 0.0009$ ) (**Figure 6B**; **Table 5**) in patients with advanced or recurrence disease. A series of survival analyses (**Figure 6C-G**) indicated that patients with high expression of *SLC25A18* may experience a longer overall survival even if they received palliative surgery treatment (HR = 0.45, 95% CI: 0.23 to 0.89,  $P = 0.0361$ ) as well as palliative systemic chemotherapy containing Bevacizumab (HR = 0.44, 95% CI: 0.22 to 0.86,  $P = 0.0307$ ).

### Discussion

Colorectal cancer is a common malignant tumor in western and eastern countries [1, 5]. Despite a median overall survival time of about 30 months, especially for advanced patients, the cause of disease recurrence and metastasis is not fully understood [25]. Characterization

## SLC25A18 inhibits Warburg effect and proliferation

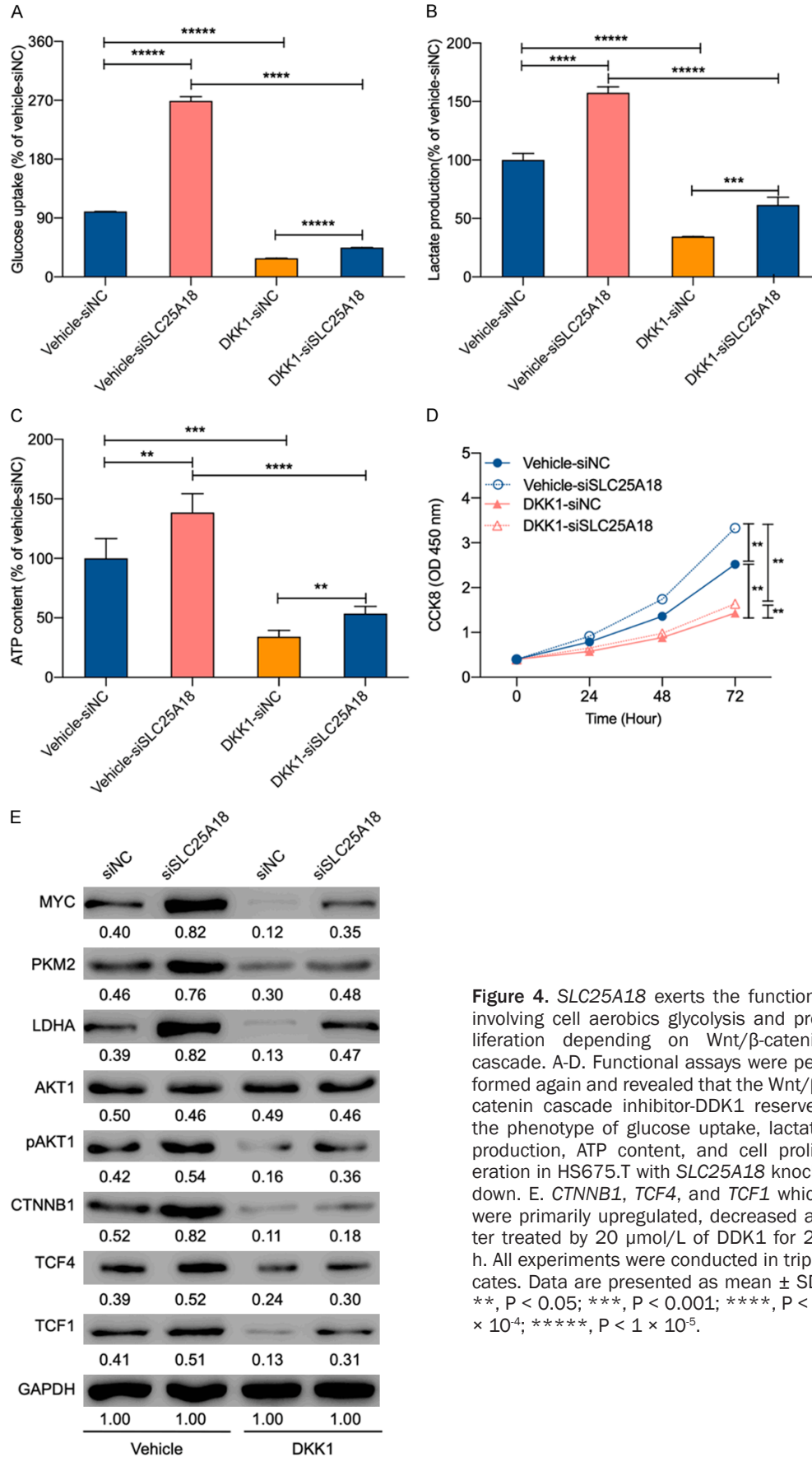


**Figure 4.** *SLC25A18* exerts the functions involving cell aerobic glycolysis and proliferation depending on Wnt/ $\beta$ -catenin cascade. A-D. Functional assays were performed again and revealed that the Wnt/ $\beta$ -catenin cascade inhibitor-DDK1 reserves the phenotype of glucose uptake, lactate production, ATP content, and cell proliferation in HS675.T with *SLC25A18* knock-down. E. *CTNNB1*, *TCF4*, and *TCF1* which were primarily upregulated, decreased after treated by 20  $\mu$ mol/L of DDK1 for 24 h. All experiments were conducted in triplicates. Data are presented as mean  $\pm$  SD. \*\*,  $P < 0.05$ ; \*\*\*,  $P < 0.001$ ; \*\*\*\*,  $P < 1 \times 10^{-4}$ ; \*\*\*\*\*,  $P < 1 \times 10^{-5}$ .

## SLC25A18 inhibits Warburg effect and proliferation

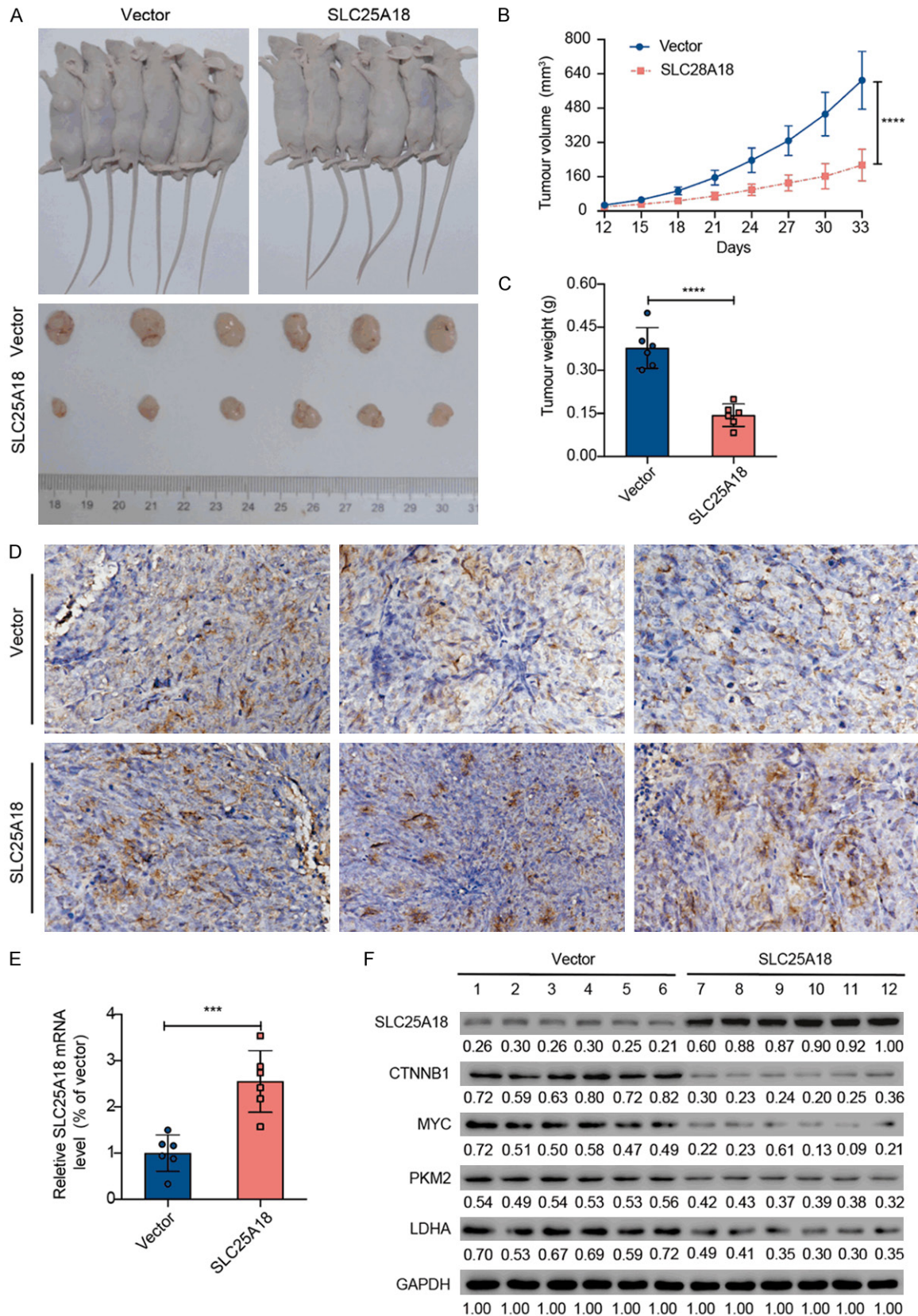


**Figure 5.** SLC25A18 attenuates CRC aerobic glycolysis in the xenograft tumor model. A. Representative photographs show subcutaneous tumor formation after implantation of HCT116 transduced with lenti-vector or lenti-

## SLC25A18 inhibits Warburg effect and proliferation

oeSLC25A18. B, C. Tumor volume and tumor weight decreased significantly in the lenti-oeSLC25A18 group. D. Positive area of SLC25A18 IHC staining was evaluated. E. RT-PCR assay confirmed the SLC25A18 expression in mRNA level. F. Western blotting assay confirmed the protein level expression of SLC25A18 as well as CTNNB1, MYC, PKM2, LDHA related to aerobic glycolysis. \*\*\*,  $P < 0.001$ ; \*\*\*\*,  $P < 1 \times 10^{-4}$ .

**Table 4.** Clinicopathological characteristics of advanced patients who receive anti-EGFR or angiogenesis target therapy and SLC25A18 expression

Clinic pathological characteristics	Number of Cases (%)	Expression level of SLC25A18 based on IHC score		P-value
		high (%)	low (%)	
Primary tumor site				0.1566
Colon	61 (59.8)	31 (50.8)	30 (49.2)	
Rectum	41 (40.2)	15 (36.6)	26 (63.4)	
Colon location				0.2806
Right	30 (29.4)	16 (53.3)	14 (46.7)	
Left	72 (70.6)	30 (41.7)	42 (58.3)	
Gender				0.8532
Male	70 (68.6)	32 (45.7)	38 (54.3)	
Female	32 (31.4)	14 (43.8)	18 (56.3)	
Age				0.0034***
≤ 60	57 (55.9)	33 (57.9)	24 (42.1)	
> 60	45 (44.1)	13 (28.9)	32 (71.1)	
Initial stage				0.7482
Advanced	55 (53.9)	24 (43.6)	31 (56.4)	
Recurrence	47 (46.1)	22 (46.8)	25 (53.2)	
Survival statuses				0.0001****
Death	48 (47.1)	12 (25.0)	36 (75.0)	
Alive	54 (52.9)	34 (63.0)	20 (37.0)	
Primary tumor resection				0.7482
Radical	55 (53.9)	24 (43.6)	31 (56.4)	
Palliative	47 (46.1)	22 (46.8)	25 (53.2)	
RAS status				0.0222**
Mutated	57 (55.9)	20 (35.1)	37 (64.9)	
Non-mutated	45 (44.1)	26 (57.8)	19 (42.2)	
RAF status				0.3625
Mutated	7(6.9)	2 (28.6)	5 (71.4)	
Non-mutated	95 (93.1)	44 (46.3)	51 (53.7)	
Anti EGFR <sup>†</sup> therapy				0.1064
Yes	40 (39.2)	22 (55.0)	18 (45.0)	
No	62 (60.8)	24 (38.7)	38 (61.3)	
Anti-angiogenesis therapy				0.049**
Yes	55 (53.9)	20 (36.4)	35 (63.6)	
No	47 (46.1)	26 (55.3)	21 (44.7)	
Total	102 (100)	46 (45.1)	56 (54.9)	

Clinical data were investigated using chi-square test. <sup>†</sup>Abbreviations: EGFR: Epidermal growth factor receptor; \*\* $P < 0.05$ ; \*\*\* $P < 0.01$ ; \*\*\*\* $P < 0.001$ .

of the biological processes and molecular mechanisms of cancer is a key focus of active investigations. According to the Warburg effect, cancer cells consume significantly more

glucose than normal cells, which means that glycolysis is still the main source of energy-ATP, even though under aerobic conditions [26-28]. As a core hallmark of cancer, metabol-

# SLC25A18 inhibits Warburg effect and proliferation

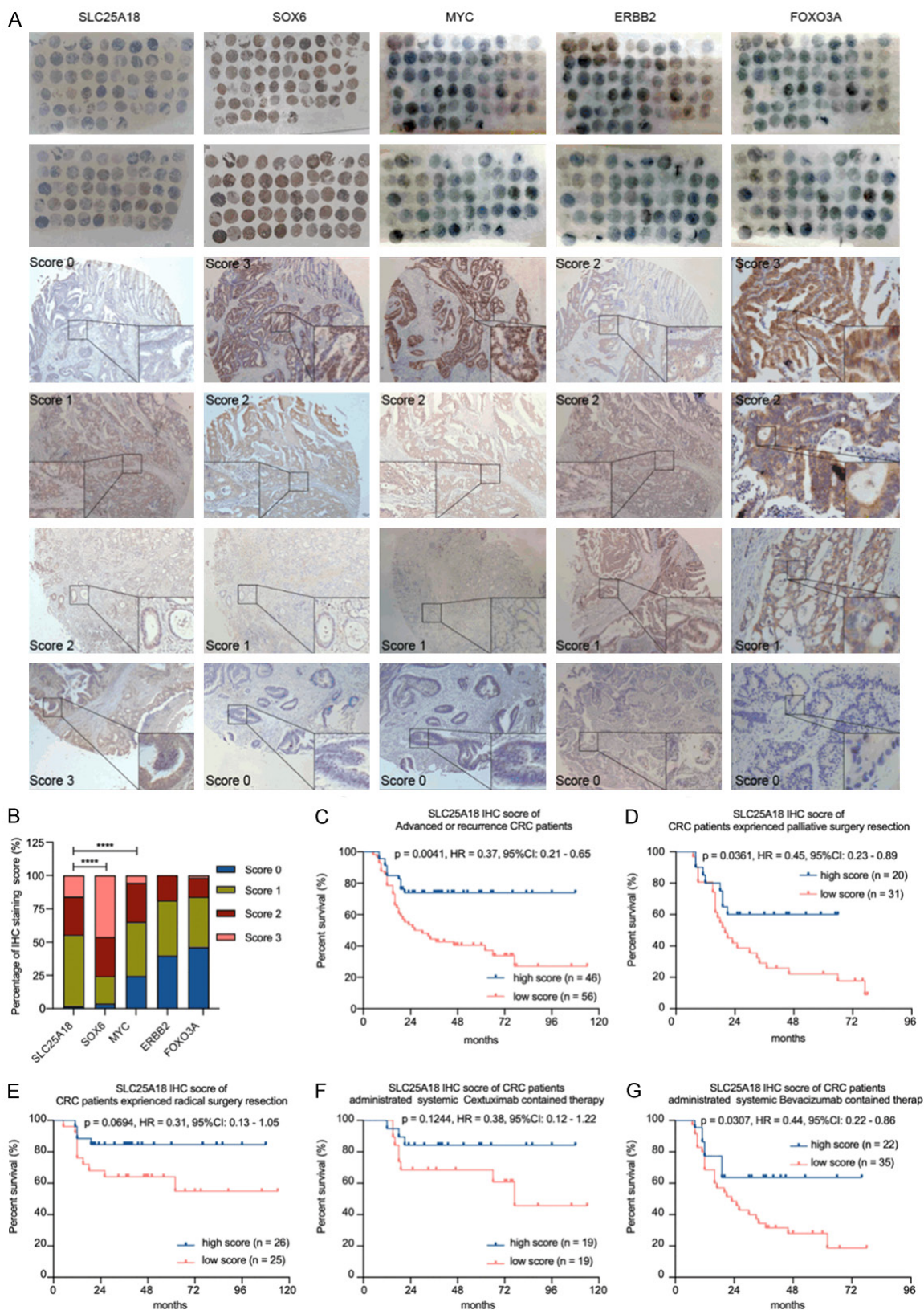


**Figure 6.** Increased SLC25A18 expression is related to a favorable prognosis in patients with CRC. A. SLC25A18, SOX6, MYC, ERBB2 and FOXO3A were examined in an immunohistochemical based tissue microarray containing 106 primary colorectal or metastatic hepatic cancer tissues. B. SLC25A18 expression level was negatively related

## SLC25A18 inhibits Warburg effect and proliferation

to some genes involving regulating aerobic glycolysis, such as *SOX6*, *MYC*. C-G. A series of survival analyses by log-rank test indicated that patients with high expression of *SLC25A18* might experience a longer survival time even if they had palliative primary resection as well as palliative systemic chemotherapy containing molecular target drug-Bevacizumab. Data are presented as mean  $\pm$  SD. \*\*\*\*,  $P < 1 \times 10^{-4}$ .

**Table 5.** Analysis of the correlation between *SLC25A18* expression and other genes by Spearman correlation test

Genes	SLC25A18 expression level		
	Spearman correlation	95% CI	P-value
<i>SOX6</i>	-0.2515	-0.4299~-0.0541	0.0108**
<i>MYC</i>	-0.3253	-0.4932~-0.1339	0.0009****
<i>ERBB2</i>	-0.1065	-0.3002~-0.0956	0.2867
<i>FOXO3A</i>	-0.0446	-0.2425~-0.1569	0.6562

\*\*P < 0.05; \*\*\*\*P < 0.001.

ic reprogramming is a way for cancer cells survival after surgical resection as well as medicine administration, which causes treatment failure in clinical practice [29]. Targeting cancer metabolism is also a new therapeutic strategy [30].

Recently, members of the SLC25 family have been widely considered as promoters of oncogenesis and disease progression [13, 31-34], especially *SLC25A22*, a paralog gene of *SLC25A18*. Knock-down of *SLC25A22* in *KRAS* mutated colon cancer could inhibit cell proliferation, invasion and migration in vitro and reduce the tumor mass growth and metastasis in xenograft models [35]. *SLC25A22* facilitates aspartic acid biosynthesis and contributes to cell proliferation and apoptosis in an aspartate amino transferase 1 dependent manner [36]. Also, *SLC25A22* contributes to malignant phenotype in gallbladder cancer and osteosarcoma [37, 38]. However, the role of *SLC25A18* in CRC has never been reported. In this study, we demonstrated that upregulation of *SLC25A18* impeded cell glucose consumption and reduced lactic acid content as well as ATP production in HCT116 and LOVO. Overexpression of *SLC25A18* also inhibited cell proliferation. Loss of function experiments suggested the opposite results in SW620 and HS675.T. The results of experiments in xenograft mice model were consistent with those in cell lines. Therefore, *SLC25A18* presents as a novel therapeutic target in CRC.

The canonical Wnt/ $\beta$ -catenin signaling pathway is involved in developmental biology of the cell and is considered a regulator of cell fate specification, cell proliferation and stem cell

pluripotency. Activation by the binding of ligand protein Wnt and membrane receptor Frizzled decreases degradation of  $\beta$ -catenin and contributes to  $\beta$ -catenin transfer into the nucleus, where it induces the expression of a series of genes regulating the cell cycle, apoptosis and epithelial-mesenchymal trans differentiation [39-44]. The disturbances between Wnt cascade and energy metabolism in osteoblasts and cardiac fibroblasts lead to osteoporosis [45] and chronic fibrosis after myocardial infarction [46]. Upregulation of Wnt/ $\beta$ -catenin signaling pathway causes aerobic glycolysis not only in non-malignant conditions such as neurodegenerative diseases [47] and mineral bone disorders [48], but also in many cancer diseases. Vallee [49] described angiogenesis and energy metabolism under normoxic conditions via Wnt/ $\beta$ -catenin in gliomas. Chin [50] indicated that Lrp5, a typical Wnt signaling receptor, has important role in glucose uptake and growth in breast cancer. Pate [51] found that inhibition of Wnt signaling reduced glycolytic metabolism and shrunk colon tumor. In this study, we found that overexpressing *SLC25A18* resulted in decrease in expression of  $\beta$ -catenin as well as enzymes that activate the Warburg effects as LDHA, PKM2, while knockdown of *SLC25A18* increased protein level of these genes. Moreover, the inhibitory effect of *SLC25A18* on the level of glucose uptake, lactic acid content, ATP production, and cell proliferation was reversed by Dickkopf inhibitor 1 (DKK1). These results suggested that the phenotype induced by *SLC25A18* is dependent on Wnt/ $\beta$ -catenin signaling pathway.

In fact, how *SLC25A18* regulating the downstream genes expression directly remains unknown. It is revealed that *SLC25A22*, also named Glutamate/H<sup>+</sup> Symporter 1, is transcribed directly by *MYC* in colorectal cancer and promotes cell proliferation and invasion by intracellular synthesis of aspartate [35]. Although our study demonstrated that *SLC25A18* regulates the expression of *MYC* and the activ-

ity of Wnt signaling pathway, we speculate that *SLC25A18* may exert a biological function by affecting the downstream metabolic network and resulting in inhibition of the oncogenesis and tumour development instead of acting as a signaling transduction. On the other hand, Riester [52] demonstrated that a failure of differentiation is the cause of stem cell-like metabolism (that is, aerobic glycolysis). Trosko [53] indicated that “stem cell theory” and the “re-programming” theory contribute to the explanation of oncogenesis, and emphasized that cancer cells have as few mitochondria as normal adult stem cell and feature persistent metabolism by the Warburg pathway. In this study, we identified a negative co-expression relationship between *SLC25A18* and stem cell like related genes such as *SOX6*, *MYC*. In support, clinical data of patients with CRC from TCGA database and GSE14333 dataset and found that *SLC25A18* was lowly expressed in CRC tissues with good clinical prognosis. The same results were confirmed in our own cohort of CRC patients. We suppose that inhibition of the Warburg effect and repression of stem cell characteristics by targeted expression of *SLC25A18* may also serve as a therapeutic strategy of cancer.

In summary, our study revealed for the first time that *SLC25A18* is downregulated in CRC tissues and presents as a biomarker of good response to anti-tumor treatment in patients with CRC. *In vivo* and *in vitro* gain- and loss-of-function experiments suggested that *SLC25A18* inhibits cell aerobic glycolysis as well as proliferation, and especially relies on Wnt/ $\beta$ -catenin signaling pathway. The potentials of *SLC25A18* acts as a promising target in cancer therapy warrants further study.

### Acknowledgements

This study was funded by grant from the Outstanding Youth Foundation of Zhongshan Hospital (No. 2019ZSYQ21) as well as National Natural Science Foundation of China (81602038, 81772511 and 81900482). We would like to thank Pro Qihong Huang's suggestion to our work.

### Disclosure of conflict of interest

None.

**Address correspondence to:** Tianshu Liu, Department of Medical Oncology, Zhongshan Hospital of Fudan University, NO. 180, Fenglin Road, Xuhui District, Shanghai 200032, China. E-mail: liu\_tianshu1969@126.com; Yingyong Hou, Department of Pathology, Zhongshan Hospital of Fudan University, Shanghai 200032, China. E-mail: hou.yingyong@zshospital.sh.cn

### References

- [1] Miller KD, Nogueira L, Mariotto AB, Rowland JH, Yabroff KR, Alfano CM, Jemal A, Kramer JL and Siegel RL. Cancer treatment and survivorship statistics, 2019. *CA Cancer J Clin* 2019; 69: 363-385.
- [2] Weinberg BA, Marshall JL and Salem ME. The growing challenge of young adults with colorectal cancer. *Oncology (Williston Park)* 2017; 31: 381-389.
- [3] Ferlay J, Steliarova-Foucher E, Lortet-Tieulent J, Rosso S, Coebergh JW, Comber H, Forman D and Bray F. Cancer incidence and mortality patterns in Europe: estimates for 40 countries in 2012. *Eur J Cancer* 2013; 49: 1374-1403.
- [4] Ferlay J, Soerjomataram I, Dikshit R, Eser S, Mathers C, Rebelo M, Parkin DM, Forman D and Bray F. Cancer incidence and mortality worldwide: sources, methods and major patterns in GLOBOCAN 2012. *Int J Cancer* 2015; 136: E359-386.
- [5] Chen W, Zheng R, Baade PD, Zhang S, Zeng H, Bray F, Jemal A, Yu XQ and He J. Cancer statistics in China, 2015. *CA Cancer J Clin* 2016; 66: 115-132.
- [6] Boland GM, Chang GJ, Haynes AB, Chiang YJ, Chagpar R, Xing Y, Hu CY, Feig BW, You YN and Cormier JN. Association between adherence to national comprehensive cancer network treatment guidelines and improved survival in patients with colon cancer. *Cancer* 2013; 119: 1593-1601.
- [7] Hines RB, Barrett A, Twumasi-Ankrah P, Broccoli D, Engelman KK, Baranda J, Ablah EA, Jacobson L, Redmond M, Tu W and Collins TC. Predictors of guideline treatment nonadherence and the impact on survival in patients with colorectal cancer. *J Natl Compr Canc Netw* 2015; 13: 51-60.
- [8] Sargent D, Sobrero A, Grothey A, O'Connell MJ, Buyse M, Andre T, Zheng Y, Green E, Labianca R, O'Callaghan C, Seitz JF, Francini G, Haller D, Yothers G, Goldberg R and de Gramont A. Evidence for cure by adjuvant therapy in colon cancer: observations based on individual patient data from 20,898 patients on 18 randomized trials. *J Clin Oncol* 2009; 27: 872-877.
- [9] Seo SI, Lim SB, Yoon YS, Kim CW, Yu CS, Kim TW, Kim JH and Kim JC. Comparison of recur-

## SLC25A18 inhibits Warburg effect and proliferation

- rence patterns between  $\leq 5$  years and  $> 5$  years after curative operations in colorectal cancer patients. *J Surg Oncol* 2013; 108: 9-13.
- [10] Wohlrab H. The human mitochondrial transport protein family: identification and protein regions significant for transport function and substrate specificity. *Biochim Biophys Acta* 2005; 1709: 157-168.
- [11] Di Noia MA, Todisco S, Cirigliano A, Rinaldi T, Agrimi G, Iacobazzi V and Palmieri F. The human SLC25A33 and SLC25A36 genes of solute carrier family 25 encode two mitochondrial pyrimidine nucleotide transporters. *J Biol Chem* 2014; 289: 33137-33148.
- [12] Porcelli V, Fiermonte G, Longo A and Palmieri F. The human gene SLC25A29, of solute carrier family 25, encodes a mitochondrial transporter of basic amino acids. *J Biol Chem* 2014; 289: 13374-13384.
- [13] Palmieri F. The mitochondrial transporter family SLC25: identification, properties and physiopathology. *Mol Aspects Med* 2013; 34: 465-484.
- [14] Palmieri F. The mitochondrial transporter family (SLC25): physiological and pathological implications. *Pflugers Arch* 2004; 447: 689-709.
- [15] Taylor EB. Functional properties of the mitochondrial carrier system. *Trends Cell Biol* 2017; 27: 633-644.
- [16] Haitina T, Lindblom J, Renstrom T and Fredriksson R. Fourteen novel human members of mitochondrial solute carrier family 25 (SLC25) widely expressed in the central nervous system. *Genomics* 2006; 88: 779-790.
- [17] Goubert E, Mircheva Y, Lasorsa FM, Melon C, Profilo E, Sutera J, Becq H, Palmieri F, Palmieri L, Aniksztejn L and Molinari F. Inhibition of the mitochondrial glutamate carrier SLC25A22 in astrocytes leads to intracellular glutamate accumulation. *Front Cell Neurosci* 2017; 11: 149.
- [18] Molinari F, Kaminska A, Fiermonte G, Boddaert N, Raas-Rothschild A, Plouin P, Palmieri L, Brunelle F, Palmieri F, Dulac O, Munnich A and Colleaux L. Mutations in the mitochondrial glutamate carrier SLC25A22 in neonatal epileptic encephalopathy with suppression bursts. *Clin Genet* 2009; 76: 188-194.
- [19] Fiermonte G, Palmieri L, Todisco S, Agrimi G, Palmieri F and Walker JE. Identification of the mitochondrial glutamate transporter. Bacterial expression, reconstitution, functional characterization, and tissue distribution of two human isoforms. *J Biol Chem* 2002; 277: 19289-19294.
- [20] Footz TK, Brinkman-Mills P, Banting GS, Maier SA, Riazi MA, Bridgland L, Hu S, Birren B, Minoshima S, Shimizu N, Pan H, Nguyen T, Fang F, Fu Y, Ray L, Wu H, Shaull S, Phan S, Yao Z, Chen F, Huan A, Hu P, Wang Q, Loh P, Qi S, Roe BA and McDermid HE. Analysis of the cat eye syndrome critical region in humans and the region of conserved synteny in mice: a search for candidate genes at or near the human chromosome 22 pericentromere. *Genome Res* 2001; 11: 1053-1070.
- [21] Fernandez-Zapico ME, van Velkinburgh JC, Gutierrez-Aguilar R, Neve B, Froguel P, Urrutia R and Stein R. MODY7 gene, KLF11, is a novel p300-dependent regulator of Pdx-1 (MODY4) transcription in pancreatic islet beta cells. *J Biol Chem* 2009; 284: 36482-36490.
- [22] Chandrashekar DS, Bashel B, Balasubramanya SAH, Creighton CJ, Ponce-Rodriguez I, Chakravarthi BVSK and Varambally S. UALCAN: a portal for facilitating tumor subgroup gene expression and survival analyses. *Neoplasia* 2017; 19: 649-658.
- [23] Warburg O. On respiratory impairment in cancer cells. *Science* 1956; 124: 269-270.
- [24] Hanahan D and Weinberg RA. Hallmarks of cancer: the next generation. *Cell* 2011; 144: 646-674.
- [25] Van Cutsem E, Cervantes A, Adam R, Sobrero A, Van Krieken JH, Aderka D, Aranda Aguilar E, Bardelli A, Benson A, Bodoky G, Ciardiello F, D'Hoore A, Diaz-Rubio E, Douillard JY, Ducreux M, Falcone A, Grothey A, Gruenberger T, Haustermans K, Heinemann V, Hoff P, Kohne CH, Labianca R, Laurent-Puig P, Ma B, Maughan T, Muro K, Normanno N, Osterlund P, Oyen WJ, Papamichael D, Pentheroudakis G, Pfeiffer P, Price TJ, Punt C, Ricke J, Roth A, Salazar R, Scheithauer W, Schmoll HJ, Tabernero J, Taieb J, Tejpar S, Wasan H, Yoshino T, Zaanan A and Arnold D. ESMO consensus guidelines for the management of patients with metastatic colorectal cancer. *Ann Oncol* 2016; 27: 1386-1422.
- [26] Schwartz L, Supuran CT and Alfarouk KO. The Warburg effect and the hallmarks of cancer. *Anticancer Agents Med Chem* 2017; 17: 164-170.
- [27] Liberti MV and Locasale JW. The Warburg effect: how does it benefit cancer cells? *Trends Biochem Sci* 2016; 41: 211-218.
- [28] Icard P, Shulman S, Farhat D, Steyaert JM, Alifano M and Lincet H. How the Warburg effect supports aggressiveness and drug resistance of cancer cells? *Drug Resist Updat* 2018; 38: 1-11.
- [29] Fumarola C, Petronini PG and Alfieri R. Impairing energy metabolism in solid tumors through agents targeting oncogenic signaling pathways. *Biochem Pharmacol* 2018; 151: 114-125.
- [30] Martinez-Outschoorn UE, Peiris-Pages M, Pestell RG, Sotgia F and Lisanti MP. Cancer metabolism: a therapeutic perspective. *Nat Rev Clin Oncol* 2017; 14: 11-31.

## SLC25A18 inhibits Warburg effect and proliferation

- [31] Palmieri F. Mitochondrial transporters of the SLC25 family and associated diseases: a review. *J Inher Metab Dis* 2014; 37: 565-575.
- [32] Ruprecht JJ and Kunji ERS. The SLC25 mitochondrial carrier family: structure and mechanism. *Trends Biochem Sci* 2020; 45: 244-258.
- [33] Lindqvist BM, Farkas SA, Wingren S and Nilsson TK. DNA methylation pattern of the SLC25A43 gene in breast cancer. *Epigenetics* 2012; 7: 300-306.
- [34] Tina E, Lindqvist BM, Gabrielson M, Lubovac Z, Wegman P and Wingren S. The mitochondrial transporter SLC25A43 is frequently deleted and may influence cell proliferation in HER2-positive breast tumors. *BMC Cancer* 2012; 12: 350.
- [35] Wong CC, Qian Y, Li X, Xu J, Kang W, Tong JH, To KF, Jin Y, Li W, Chen H, Go MY, Wu JL, Cheng KW, Ng SS, Sung JJ, Cai Z and Yu J. SLC25A22 promotes proliferation and survival of colorectal cancer cells with KRAS mutations and xenograft tumor progression in mice via intracellular synthesis of aspartate. *Gastroenterology* 2016; 151: 945-960, e946.
- [36] Xie J, Zhu XY, Liu LM and Meng ZQ. Solute carrier transporters: potential targets for digestive system neoplasms. *Cancer Manag Res* 2018; 10: 153-166.
- [37] Du P, Liang H, Fu X, Wu P, Wang C, Chen H, Zheng B, Zhang J, Hu S, Zeng R, Liang B and Fang L. SLC25A22 promotes proliferation and metastasis by activating MAPK/ERK pathway in gallbladder cancer. *Cancer Cell Int* 2019; 19: 33.
- [38] Chen MW and Wu XJ. SLC25A22 promotes proliferation and metastasis of osteosarcoma cells via the PTEN signaling pathway. *Technol Cancer Res Treat* 2018; 17: 1533033818811143.
- [39] Cadigan KM and Waterman ML. TCF/LEFs and Wnt signaling in the nucleus. *Cold Spring Harb Perspect Biol* 2012; 4.
- [40] Clevers H and Nusse R. Wnt/beta-catenin signaling and disease. *Cell* 2012; 149: 1192-1205.
- [41] Valenta T, Hausmann G and Basler K. The many faces and functions of beta-catenin. *EMBO J* 2012; 31: 2714-2736.
- [42] Nagano H, Hashimoto N, Nakayama A, Suzuki S, Miyabayashi Y, Yamato A, Higuchi S, Fujimoto M, Sakuma I, Beppu M, Yokoyama M, Suzuki Y, Sugano S, Ikeda K, Tatsuno I, Manabe I, Yokote K, Inoue S and Tanaka T. p53-inducible DPYSL4 associates with mitochondrial supercomplexes and regulates energy metabolism in adipocytes and cancer cells. *Proc Natl Acad Sci U S A* 2018; 115: 8370-8375.
- [43] Zeve D, Seo J, Suh JM, Stenesen D, Tang W, Berglund ED, Wan Y, Williams LJ, Lim A, Martinez MJ, McKay RM, Millay DP, Olson EN and Graff JM. Wnt signaling activation in adipose progenitors promotes insulin-independent muscle glucose uptake. *Cell Metab* 2012; 15: 492-504.
- [44] Rharass T, Lemcke H, Lantow M, Kuznetsov SA, Weiss DG and Panakova D. Ca<sup>2+</sup>-mediated mitochondrial reactive oxygen species metabolism augments Wnt/beta-catenin pathway activation to facilitate cell differentiation. *J Biol Chem* 2014; 289: 27937-27951.
- [45] Yao Q, Yu C, Zhang X, Zhang K, Guo J and Song L. Wnt/beta-catenin signaling in osteoblasts regulates global energy metabolism. *Bone* 2017; 97: 175-183.
- [46] Lin H, Angeli M, Chung KJ, Ejimadu C, Rosa AR and Lee T. sFRP2 activates Wnt/beta-catenin signaling in cardiac fibroblasts: differential roles in cell growth, energy metabolism, and extracellular matrix remodeling. *Am J Physiol Cell Physiol* 2016; 311: C710-C719.
- [47] Vallee A, Lecarpentier Y, Guillevin R and Vallee JN. Thermodynamics in neurodegenerative diseases: interplay between canonical WNT/Beta-catenin pathway-PPAR gamma, energy metabolism and circadian rhythms. *Neuromolecular Med* 2018; 20: 174-204.
- [48] de Oliveira RB, Gracioli FG, dos Reis LM, Cancela AL, Cuppari L, Canziani ME, Carvalho AB, Jorgetti V and Moyses RM. Disturbances of Wnt/beta-catenin pathway and energy metabolism in early CKD: effect of phosphate binders. *Nephrol Dial Transplant* 2013; 28: 2510-2517.
- [49] Vallee A, Guillevin R and Vallee JN. Vasculogenesis and angiogenesis initiation under normoxic conditions through Wnt/beta-catenin pathway in gliomas. *Rev Neurosci* 2018; 29: 71-91.
- [50] Chin EN, Martin JA, Kim S, Fakhraldeen SA and Alexander CM. Lrp5 has a Wnt-independent role in glucose uptake and growth for mammary epithelial cells. *Mol Cell Biol* 2015; 36: 871-885.
- [51] Pate KT, Stringari C, Sprowl-Tanio S, Wang K, TeSlaa T, Hoverter NP, McQuade MM, Garner C, Digman MA, Teitell MA, Edwards RA, Gratton E and Waterman ML. Wnt signaling directs a metabolic program of glycolysis and angiogenesis in colon cancer. *EMBO J* 2014; 33: 1454-1473.
- [52] Riestler M, Xu Q, Moreira A, Zheng J, Michor F and Downey RJ. The warburg effect: persistence of stem-cell metabolism in cancers as a failure of differentiation. *Ann Oncol* 2018; 29: 264-270.
- [53] Trosko JE and Kang KS. Evolution of energy metabolism, stem cells and cancer stem cells: how the warburg and barker hypotheses might be linked. *Int J Stem Cells* 2012; 5: 39-56.